7-2010

Noxa mediates hepatic stellate cell apoptosis by proteasome inhibition.

Ivette M. Sosa Seda
Mayo Clinic

Justin L. Mott
University of Nebraska Medical Center, justin.mott@unmc.edu

Yuko Akazawa
Mayo Clinic

Fernando J. Barreyro
Mayo Clinic

Steven F. Bronk
Mayo Clinic

See next page for additional authors

Published in final edited form as:
Hepatol Res. 2010 July 1; 40(7): 701–710. doi:10.1111/j.1872-034X.2010.00668.x.

Noxa Mediates Hepatic Stellate Cell Apoptosis by Proteasome Inhibition

Ivette M. Sosa Seda[1,2], **Justin L. Mott**[1], **Yuko Akazawa**[1], **Fernando J. Barreyro**[1], **Steven F. Bronk**[1], **Scott H. Kaufmann**[3], and **Gregory J. Gores**[1]

[1]Division of Gastroenterology and Hepatology, Mayo Clinic College of Medicine, Rochester, Minnesota 55905

[2]University of Puerto Rico, School of Medicine, San Juan, Puerto Rico 00926

[3]Division of Oncology Research, College of Medicine, Mayo Clinic, Rochester, MN 55905

Abstract

Aim—Induction of hepatic stellate cell (HSC) apoptosis is a viable therapeutic strategy to reduce liver fibrogenesis. Although BH3-only proteins of the Bcl-2 family trigger pro-apoptotic pathways, the BH3-only proteins mediating HSC apoptosis have not been well defined. Our aim, using proteasome inhibition as a model to induce HSC apoptosis, was to examine the BH3-only proteins contributing to cell death of this key liver cell subtype.

Methods—Apoptosis was induced by treating LX-2 cells, an immortalized human hepatic stellate cell line, and primary rat stellate cells with the proteasome inhibitor MG-132.

Results—Treatment with proteasome inhibitors increased expression of Noxa both at the mRNA (16-fold) and protein (22-fold) levels indicating that both transcriptional and post-translational mechanisms contributed to the increase in cellular Noxa levels. Knockdown of Noxa by siRNA significantly attenuated cell death, mechanistically implicating Noxa as a key apoptotic mediator of proteasome inhibitor-induced cell death. Given the pivotal role for the anti-apoptotic Bcl-2 protein A1 in activated HSC survival, we determined if Noxa bound to this survival protein. Noxa was shown to physically bind the anti-apoptotic Bcl-2 protein A1 by co-immunoprecipitation.

Conclusions—Noxa contributes to proteasome inhibitor-induced apoptosis of stellate cells likely by binding A1. Strategies to therapeutically increase Noxa expression may be useful for inducing HSC apoptosis.

Keywords

BCL2-related protein A1; Bfl-1; BH3-only proteins; Fibrosis; PMAIP1; S-peptide

INTRODUCTION

Hepatic stellate cells (HSCs) are the principle source of hepatic collagen, and therefore, play a critical role in the development and maintenance of hepatic fibrosis, a nefarious consequence of all chronic liver diseases regardless of etiopathogenesis[1, 2]. In health, HSCs store retinoids and generate little if any collagen3. In response to hepatic injury, these cells transform into a myofibroblast phenotype and secrete collagen. HSCs appear to undergo a commitment step to become activated and undergo limited reversion to the quiescent

Address correspondence to: Gregory J. Gores, M.D. Mayo Clinic, 200 First Street SW, Rochester, Minnesota 55905, USA, Phone: (507) 284-0686, Fax: (507) 284-0762, gores.gregory@mayo.edu.

phenotype *in vivo*. Analogous to activation-induced cell death of T-lymphocytes4, activated HSCs are eliminated by apoptosis5–7. Thus, reversal and/or inhibition of hepatic fibrosis requires HSC apoptosis. In support of this concept, compounds which inhibit NF-κB activation (a transcription factor which promotes HSC survival), such as gliotoxin or sulfasalazine, and the proteasome inhibitor bortezomib reduce hepatic fibrosis by inducing HSC apoptosis8–11. Information regarding the cellular and molecular mechanisms regulating HSC apoptosis is limited, however, impeding the development of anti-fibrotic strategies based on inducing therapeutic HSC apoptosis.

The intrinsic pathway of apoptosis converges on mitochondria resulting in mitochondrial outer membrane permeabilization with efflux of cytochrome c and other proapoptotic proteins into the cytosol12. Once in the cytosol, these proteins promote caspase activation which in turn causes cellular demise13. The mitochondrial pathway of apoptosis is regulated by members of the Bcl-2 family of proteins14. Members of this family with up to four Bcl-2 homology (BH) domains, such as Bcl-2, Bcl-X_L, Mcl-1 and A1, function as guardians of the mitochondria preventing apoptosis15. The multidomain executioners of mitochondrial dysfunction are Bax and Bak16, 17 which directly induce mitochondrial dysfunction by permeabilizing the outer mitochondrial membrane18. The Bcl-2 proteins displaying sequence homology exclusively in the short BH3 domain are referred to as BH3-only proteins. These proteins are biosensors of cellular stress and induce apoptosis by functioning as intracellular death ligands, including Bad, Bid, Bik, Bim, Bmf, Hrk, Noxa and Puma19. The mechanisms by which they induce cell death remain unresolved, but include direct ligation and activation of Bax and/or Bak, inhibition of anti-apoptotic multi-domain Bcl-2 proteins, or both14. By whatever mechanism they induce cell death, BH3-only proteins are critical upstream mediators of the cell death program. The constellation of BH3-only proteins regulating cell death vary between cell types and remain incompletely understood in HSCs.

We have employed proteasome inhibitors as a model to help elucidate which Bcl-2 proteins regulate HSC apoptosis. Proteasome inhibitors rapidly induce apoptosis by complex mechanisms20. First, these agents prevent NF-κB activation, a transcription factor necessary for maximal expression of the anti-apoptotic multidomain Bcl-2 protein A121. Indeed, A1 is an important survival protein for activated HSCs as inhibition of its expression by targeted siRNA is sufficient to induce cell death of this cell type10. However, the BH3-only proteins participating in this process remain unclear. Although protease inhibitors enhance Bim expression, inhibition of Bim by siRNA technology does not reduce HSC apoptosis by proteasome inhibition10. Another BH3-only protein induced by proteasome inhibitors is Noxa22–26. Noxa is an attractive BH3-only protein inducing HSC apoptosis given its potential ability to bind A1 *in vitro*27. However, information is lacking regarding a potential role for Noxa in mediating apoptosis of HSC cells.

MATERIAL AND METHODS

Cell lines and culture

The human stellate cell line, LX-2 cells were obtained from Dr. Scott Friedman, Mt. Sinai, NY28. LX-2 cells were cultured in Dulbecco's Modified Eagle Medium (DMEM, GIBCO, Invitrogen, Grand Island, NY) containing high glucose (25 mM), 100,000 units/L penicillin, 100 mg/L streptomycin and 10% fetal bovine serum. Primary rat HSCs were isolated and cultured as previously described10.

Quantification of apoptosis

Apoptosis was quantified morphologically by assessing the characteristic nuclear changes using the DNA binding dye 4′,6-diamidino-2-phenylindole (DAPI, Molecular Probes Inc., Eugene, OR) as previously described by us[29]. Apoptosis was also verified biochemically by measuring caspase 3/7 activity. Briefly, cells were plated in a 96-well plate (Corning Inc., Corning, NY). Caspase-3/7 activity in LX-2 cells was quantified utilizing the commercially available Apo-ONE detection assay kit (Apo-ONE homogeneous caspase-3/7 assay, Promega Corporation, Madison, WI) according to the manufacturer's instructions. Fluorescence intensity was measured using a fluorescence plate reader FLx 800 Microplate (BIO-TEK Instruments, Winooski, Vermont). The amount of fluorescent product generated is proportional to the amount of caspase-3/7 cleavage activity present in the sample and is expressed as RFU (Relative Fluorescence Units).

Immunoblot analysis

Whole cell lysates were obtained as previously described by us in detail[30]. Protein concentration of the supernatant was determined by the Bradford assay (Bio-Rad, Hercules, CA). Proteins were electrophoretically resolved by 15% SDS-PAGE and immobilized on a nitrocellulose membrane. Membranes were blocked in 5% non-fat dairy milk in Wash buffer (TBS-T; 20 mM Tris, pH 7.4, 150 mM NaCl, 0.1% Tween-20) was employed. Blots were incubated with primary antibodies at 4°C overnight and with secondary antibodies at room temperature for 1 hour. The following primary antibodies were used: mouse anti-hNoxa monoclonal antibody (114C307.1, dilution 1:1000, Alexis Biochemicals, Axxora Platforms, San Diego, CA), rat anti-Bim monoclonal antibody (MAB17001, 1:1000, Chemicon, Milipore Corporation, Billerica, MA), rabbit anti-Puma polyclonal antibody (3043, 1:1000, Prosci Incorporated, Poway, CA), goat anti-Bid polyclonal antibody (AF860, 1:1000, R&D System, Minneapolis, MN), rabbit anti-Bad polyclonal antibody (sc-7869, 1:1000, Santa Cruz Biotechnology, Santa Cruz, CA), goat anti-actin polyclonal antibody (sc-1615, 1:2000, Santa Cruz Biotechnology), rabbit anti-Bik polyclonal antibody (sc-10770, 1:1000, Santa Cruz Biotechnology), rabbit anti-Bak polyclonal antibody (sc-832, 1:1000, Santa Cruz Biotechnology), rabbit anti-S-probe polyclonal antibody (sc-802, 1:1000, Santa Cruz Biotechnology), and finally, mouse monoclonal antibody to α-tubulin (T6557, 1:5000, Sigma Pharmaceuticals, St. Louis, MO). Peroxidase-conjugated secondary antibodies (dilution 1:3000, Biosource International, Camarillo, CA) were used to detect antigen-antibody complexes. These complexes were visualized using enhanced chemiluminescent substrate (ECL, Amersham, Arlington Heights, IL) and were exposed to Kodak X-OMAT films (Eastman Kodak, Rochester, NY). Either actin or α-tubulin were used as loading controls.

Reverse Transcription Polymerase Chain Reaction (RT-PCR)

Total RNA was isolated using TRIzol reagent (Invitrogen, Carlsbad, CA), and reverse-transcribed using random primers and Moloney leukemia virus reverse transcriptase (Invitrogen, Carlsbad, CA). PCR primers used for human Noxa were as follows: forward 5'-GCA GAG CTG GAA GTC GAG TG-3' and reverse 5'-AGC AGA AGA GTT TGG ATA TCA G-3' (yielding a 101 bp-product). Commercially available primers for ribosomal 18S RNA (Ambion, Austin, TX) were used as internal controls. Quantification of the complementary DNA template was performed with real-time polymerase chain reaction using the Light Cycler (Roche Molecular Biochemicals, Mannheim, Germany) as we have previously described in detail[29].

Noxa mRNA and protein half-life

To examine the effect of proteasome inhibition on the half-life of Noxa mRNA, LX-2 cells were treated with media and vehicle containing 10 μmol/L MG-132 (Calbiochem, CA) in the presence or absense of 5 μmol/L actinomycin D (Sigma-Genosys, Woodlands, TX). Using this approach, at each selected time interval, total cellular RNA was isolated for RT-PCR of Noxa. To examine the effect of the proteasome inhibition on the half-life of Noxa protein, LX-2 cells were treated with vehicle in the presence and absence of MG-132 plus cyclohexamide 20 μg/ml for 0–8 hours. At the selected time interval, cells were lysed, and the lysates subjected to immunoblot analysis for Noxa as described above. Noxa and actin bands were quantified as previously described by us in detail[31]. The half-life was determined by $t_{1/2} = \ln(2)/\lambda$, where λ is the decay constant.

Small interfering RNA (siRNA) experiments

RNA interference was used to silence Noxa gene expression in LX-2 cells. Noxa siRNA sense 5'-GGA GAU UUG GAG ACA SAA CUtt-3' and anti-sense 3'-AGU UUG UCU CCA AAU CUC Ctg-5' were purchased from Ambion (Austin, TX). Transient gene silencing was attained by transfection of siRNA into cells using siPORT lipid transfection reagent (Ambion) according to the manufacturer's instructions. Scrambled siRNA was used as control. Cells were transiently transfected in 6-well plates at 30% confluency. We used a final concentration of 100 nM Noxa siRNA by using 6 μL of siPORT lipid in a total transfection volume of 1 mL of OPTIMEM (Gibco-Invitrogen Corporation, Carlsbad, CA). After 3 hours of transfection, 1.5 ml of medium per well was added.

Stable transfection of S-peptide-tagged human A1 expression plasmid

The human A1 cDNA was amplified from HEL cells by rt-PCR (forward primer 5'-GTATCTGGTACCACAGACTGTGAATTTGGATAT-3 ', reverse primer 5 '-GCTACTGAATTCTCAACAGTATTGCTTCAGG-3') and subcloned into the KpnI and EcoRI sites of pSPN to yield the S peptide epitope tag fused to the N terminus of A132. The plasmid was subjected to nucleotide sequencing for confirmation. An S-peptide epitope tag was then added as previously described by us31. The plasmid was subjected to nucleotide sequencing for confirmation. Transfection with the S-peptide-tagged A1 expression plasmid was performed using a standard lipofectamine method (Life Technologies, Inc., Gaithersburg, MD). Stably transfected LX-2 clones were selected in medium containing 1200 μg/ml G418. Individual colonies were sub-cloned and screened for A1 protein expression by immunoblot analysis for the s-peptide tag. Established clones were grown in DMEM supplemented with 10% fetal bovine serum, 10% bovine calf serum, 100,000 units/L penicillin, 100 mg/L streptomycin, and 1200 mg/L G418.

Affinity purification of S-peptide-tagged A1

Cells were lysed in buffer containing 50 mm Tris (pH 7.4), 150 mM NaCl, 1 mM EDTA, 1mM PMSF, 1mM Na3VO4, 100mM NaF, 20 mM microcystin, 2% CHAPS and Complete Protease Inhibitor as per manufactures protocol. Lysates (1 mL) were centrifuged at 13000 *g* for 15 minutes to eliminate insoluble matter. Supernatant was transferred to fresh tubes and 100 μL of S-protein Agarose (Novagen) was added. Samples were gently agitated overnight at 4°C. Samples were centrifuged at 10000 *g* for 1 min and supernatent discarded. Remaining S-agarose was washed 6 times with 1 mL volumes of the previous lysis buffer minus CHAPS. Following the final wash an equal volume (100 μL) of 2X Laemmli sample buffer was added. Samples were boiled for 10 minutes and resolved by SDS-PAGE and subjected to immunoblot analysis as described above.

Immunocytochemistry

Cells were cultured on 6 well plates containing coverslips. After the treatment, the medium was aspirated, and the cells were washed 3 times with phosphate-buffered saline (PBS) and then fixed with 4% paraformaldehyde in PBS containing 0.1 m PIPES, 1 mm EGTA, and 3 mm $MgSO_4$ for 15 min at 37 °C. After the second wash with PBS, cells were permeabilized using 0.0125% (w/v) CHAPS in PBS at room temperature for 15 min. Cells were then incubated in PBS containing 5% goat serum at room temperature for an hour. After incubation with rabbit anti-Bak NT antisera (1:300 Upstate, Lake Placid, NY) overnight at 4 °C, cells were washed 3 times with PBS and incubated with Alexa Fluor 488-conjugated goat anti-rabbit IgG (Molecular Probes) for 1 h at 37 °C. Cells were then washed 3 times in PBS and 3 times in H_2O, mounted onto slides using a ProLong Antifade kit with DAPI (Molecular Probes), and imaged by confocal microscopy with excitation and emission wavelengths of 488 and 505–580 nm (Alexa Fluor 488) and 364 and 385–470 nm (DAPI), respectively.

Reagents

DAPI, OPH-19 Q-VD-OPH, MG-132 in solution (474791) and inhibitor Bay 11–70829 were purchased from Calbiochem (La Jolla, CA). Cyclohexamide and actinomycin D (A9415) were from Sigma Pharmaceuticals (St. Louis, MO). S-protein agarose (69704) was purchased from Novagen, (San Diego, CA).

Data analysis

All data are expressed as the mean ± standard error of the mean (SEM), representing at least three separate experiments, unless otherwise specified. Analysis of variance (ANOVA) was used for comparing differences between groups and to correct for multiple comparisons, a Bonferroni post-hoc correction was employed. A p value less than 0.05 was considered statistically significant. All statistical analyses were performed using In-Stat Software (Graph Pad, San Diego, CA).

RESULTS

MG-132 treatment induce expression of Noxa protein

The proteasome inhibitor MG-132 induced apoptosis in the human HSC, LX-2 cell line, in a time- and concentration-dependent manner (Fig. 1A and B). Maximal apoptosis was 50–60% after 24 hour treatment with MG-132, 10 μmol/L. M G-132 cytotoxicity was caspase-dependent as it was completely abrogated by the pan-caspase inhibitor QVD (Fig. 1A). Having established the time course and the dose dependence for MG-132-mediated LX-2 cells apoptosis, we next examined the cellular expression of BH3-only proteins. Noxa, Bim, Puma, Bad and Bid were expressed at the protein level in LX-2 cells (Fig. 2A). In contrast, protein expression of Bmf, Hrk and Bik was not detected by immunoblot analysis. Protein levels of Noxa and Bim increased after exposure of the cells to MG-132 (Fig. 2A). In particular, Noxa protein levels increased by 22-fold, as measured by densitometric analysis of immunoblots from triplicate experiments. This expression of Noxa by MG-132 treatment was observed not only in LX-2 cells but also in isolated rat primary HSCs (Fig 2B). Since we have previously demonstrated that inhibiting Bim expression by siRNA did not prevent MG-132-mediated apoptosis[10], we focused the remainder of this study on the role of Noxa in apoptosis by MG-132.

Noxa is up-regulated by transcriptional and post-transcriptional mechanisms

In addition to the increase in Noxa cellular protein levels during proteasome inhibition, we also observed a 16-fold increase in steady state Noxa mRNA (Fig. 3). To ascertain whether

MG-132 increased Noxa mRNA steady state levels by stabilizing Noxa mRNA, its half-life was quantified in the presence of the transcription inhibitor, actinomycin D. MG-132 treatment of LX-2 cells did not increase the half-life of Noxa mRNA (Fig. 4A). Thus, in the absence of Actinomycin D, MG-132 increased Noxa mRNA levels by 16-fold, while in the presence of the transcriptional inhibitor, cells treated with MG-132 did not have higher Noxa mRNA levels than control (the slight decrease compared to control cells, 26% at 6 hours, was not statistically significant). Thus *de novo* transcription was required in order to observe increased Noxa mRNA levels in MG-132 treated cells compared to control, suggesting the increase in steady state mRNA reflected enhanced transcription. Consistent with its ability to block degradation of proteins by the proteasome, MG-132 prolonged the half-life of Noxa protein (Fig. 4B). The calculated half-life of Noxa protein was 22 minutes, which was increased up to 20 hours in the presence of MG-132. Thus, proteasome inhibition appears to increase cellular levels of Noxa by both transcriptional and post-transcriptional mechanisms.

Noxa is essential for apoptosis by proteasome inhibition

To ascertain if Noxa is essential for mediating MG-132 apoptosis, its protein expression was knocked down using siRNA technology. First, we verified the efficacy and specificity of the siRNAs targeting Noxa. Indeed, its protein level was reduced 92% by this siRNA during proteasome treatment (Fig. 5A). Knock down of Noxa was specific as cellular protein levels of Bim were unaltered. Having demonstrated the efficacy of Noxa siRNA in reducing Noxa cellular protein levels, cells transfected with Noxa siRNA were treated with MG-132 and apoptosis was quantified. LX-2 cells transfected with Noxa siRNA demonstrated a reduction of 54% in MG-132 cytotoxicity by both morphologic criteria and caspase-3/7 activity (Fig. 5A and 5B). In contrast, scrambled siRNA-transfected cells were not protected against MG-132 cytotoxicity. Taken together, these data suggest that MG-132-induced apoptosis is, in part, Noxa-dependent.

A1 partially protects LX-2 cells from apoptosis by MG-132

We have previously reported that proteasome inhibition decreased A1 mRNA expression in LX-2 cells, and further that A1 gene silencing by siRNA induced LX-2 cell death[10]. Thus, A1 acts as a mediator of LX-2 survival. To determine whether enforced expression of A1 was sufficient to protect cells treated with MG-132, we measured apoptosis in LX-2 cells stably transfected with an A1 expression plasmid (termed LX-2/A1). Compared to parental cells, LX-2/A1 cells had partial protection from MG-132-induced apoptosis (Fig. 6A). However, protection was only partial, suggesting that A1 is functionally inhibited in cells treated with MG-132.

Noxa associates with A1 upon MG-132 treatment

It has been proposed that anti-apoptotic Bcl-2 proteins such as A1 are functionally neutralized following binding by BH3-only proteins[27]. Based on this model, we considered that the anti-apoptotic activity of A1 may be inhibited by binding to Noxa. We employed LX-2/A1 cells stably expressing S peptide-tagged A1 to ensure adequate A1 expression as well as providing an epitope tag to facilitate pulldown, given previous difficulty in using commercial antibodies for A1 immunoprecipitation. The ability of A1 to bind Noxa was then examined as described under the experimental procedure section. Affinity purification of S peptide-tagged A1 from whole cell lysates revealed binding of Noxa to this anti-apoptotic protein following treatment of LX-2 cells with MG-132 (Fig. 6B). These data are compatible with neutralization of A1 by Noxa.

A1, in part, antagonizes cell death signals by binding to the pro-apoptotic, multidomain, Bcl-2 protein Bak[14]. Therefore, we postulated that if Noxa binds A1 disabling its function,

Bak would not bind as efficiently to A1. To test the A1:Bak interaction we utilized affinity purification of S peptide-tagged A1, as above, and probed the pulldown with antiserum specific for Bak. In vehicle-treated cells, A1 and Bak could be co-precipitated (Fig. 6C). We observed a increase in S-peptide tagged A1 protein levels upon MG-132 treatment in this experiment, possibly due to decreased degradation of A1 by the proteasome. When LX-2/A1 cells were treated with MG-132, both polypeptides were recoved in higher amounts, however the Bak/A1 ratio was decreased compared to vehicle. One interpretation of these data is that Noxa binding to A1 decreased the Bak/A1 ratio, permiting Bak derepression and activation.

We next investigated Bak activation in LX-2 cells treated with MG-132. Activation of Bak can be visualized by immunofluorescent staining utilizing antiserum specific for the N terminal of Bak. This epitope is normally not accessible to the antibody for binding, however, upon activation, Bak undergoes a conformational change facilitating staining by the N terminal-specific Bak antibody[33]. Indeed, we observed Bak activation in MG-132 treated LX-2 cells (Fig. 6D). Taken together, these data further implicate Noxa inhibition of A1 as a mechanism contributing to stellate cell death by proteasome inhibitors.

DISCUSSION

The results of this study provide new insight into the mechanisms of stellate cell apoptosis. The results indicate that during pharmacologic proteasome inhibition: i) Noxa protein levels are increased by both transcriptional and post-translational mechanisms; ii) siRNA targeted knock down of Noxa attenuates apoptosis and iii) Noxa likely exerts its pro-apoptotic activity, in part, by binding to the anti-apoptotic protein A1 thus derepressing Bak. Each of these results is discussed in greater detail below.

Proteasome inhibition has been previously demonstrated to reduce liver injury, attenuate hepatic fibrosis, and induce stellate cell apoptosis *in vivo* and *in vitro*, respectively10, 11. Therefore, we employed cultured HSC to continue our exploration of the mechanisms modulating HSC apoptosis. The current study focused on the BH3-only proteins involved in triggering apoptosis, as these proteins act as biosensors of cell stress and initiate the critical cellular cascades culminating in cellular demise. Of the five BH3-only proteins expressed by LX-2 cells, only two increased during proteasome inhibitor triggered apoptosis, Bim and Noxa. We have previously demonstrated that siRNA knockdown of Bim was insufficient to attenuate apoptosis in this model10; therefore, Noxa appears to be the primary BH3-only protein contributing to HSC apoptosis in this model. The increase in Noxa following proteasome inhibition was associated with an increase both in its mRNA and protein half-life. These observations suggest proteasome inhibition increases cellular Noxa levels by both transcriptional and post-translational mechanisms. Although p53 is a potent inducer of Noxa, its increase during proteasome inhibition is p53-independent[34]. Wang and co-workers have recently demonstrated that proteasome inhibition induces endoplasmic reticulum stress (unfolded protein response) which increases Noxa transcription via the transcription factors ATF3 and ATF4[35]. Fernandez et al. have also suggested that proteasome inhibition extends the half-life of Noxa22, an assumption which we were able to directly confirm. Collectively, these composite observations suggest the increase of cellular Noxa levels during proteasome inhibition is multifactorial. The concept that endoplasmic reticulum stress is a potent inducer of Noxa suggests that this mechanism of inducing Noxa and hence stellate cell apoptosis warrants further therapeutic exploration.

siRNA targeted knockdown of Noxa reduced LX-2 apoptosis by the proteasome inhibitor MG-132. Prior studies have also implicated Noxa as a key mediator of apoptosis in cancer cells during proteasome inhibition[22, 23, 26, 34–36]. Thus, activated stellate cells appear to

respond to proteasome inhibition much like transformed cells. This observation gives credence to the concept that when activated, stellate cells assume many features of transformed cells with enhanced proliferation, ability to migrate, and differential sensitivity to pro-apoptotic stimuli[3].

We have previously demonstrated that survival of activated LX-2 cells is dependent upon expression of the pro-apoptotic protein A1. BH3-only proteins differentially bind to pro-apoptotic proteins[14], and Noxa peptides demonstrate high affinity binding to Mcl-1 and A1 in vitro[27]. We have extended these observations by demonstrating for the first time to our knowledge binding of Noxa protein to A1 in a cellular context. Upon binding BH3-only proteins, anti-apoptotic proteins such as A1 lose their ability to repress activation of pro-apoptotic multidomain proteins, such as Bak[14]. Given this information, Noxa likely triggers apoptosis, in part, by binding to and inhibiting the pro-survival effect of A1 on Bak. Indeed, the Bak/A1 ratio was decreased in cells upon MG-132 treatment while Bak activation was increased. It remains possible that Noxa promotes Bak activation by additional, as yet unknown, mechanisms.

Inducing stellate cell apoptosis remains a viable therapeutic strategy for treating hepatic fibrosis[37]. Our current studies suggest that approaches to enhance Noxa expression facilitate apoptosis induction in this liver cell type. Noxa likely promotes stellate cell apoptosis by binding A1, a dominant pro-survival protein for these cells. Other cellular events likely also contribute to cellular demise in this model of cell death by proteasome inhibition. Therefore, it will be necessary to confirm these observations in other models, but if our results are confirmed in additional models, stellate cell specific Noxa expression may provide a foundation for the development of new therapeutic approaches for hepatic fibrosis.

Acknowledgments

The authors thank Erin Nystuen-Bungum for her excellent secretarial assistance. We also gratefully acknowledge Nga Dai who constructed the S peptide-tagged A1 plasmid.

Grants: This work was supported by student research fellowship award from the American Gastroenterological Association Foundation, grant R25 GM 75148 by the National Institutes of Health (NIH) to Initiative to Maximize Student Diversity (IMSD) program to I.M.S.S., and by NIH grants DK 41876 (G.J.G.), and CA 69008 (S.H.K), as well as the Mayo Foundation Rochester, MN.

REFERENCES

1. Friedman SL. Seminars in medicine of the Beth Israel Hospital, Boston. The cellular basis of hepatic fibrosis. Mechanisms and treatment strategies. N Engl J Med 1993;328(25):1828–1835. [PubMed: 8502273]
2. Friedman SL. Molecular regulation of hepatic fibrosis, an integrated cellular response to tissue injury. J Biol Chem 2000;275(4):2247–2250. [PubMed: 10644669]
3. Friedman SL. Hepatic stellate cells: protean, multifunctional, and enigmatic cells of the liver. Physiol Rev 2008;88(1):125–172. [PubMed: 18195085]
4. Krammer PH, Arnold R, Lavrik IN. Life and death in peripheral T cells. Nat Rev Immunol 2007;7(7):532–542. [PubMed: 17589543]
5. Arthur MJ. Reversibility of liver fibrosis and cirrhosis following treatment for hepatitis C. Gastroenterology 2002;122(5):1525–1528. [PubMed: 11984538]
6. Iredale JP. Hepatic stellate cell behavior during resolution of liver injury. Semin Liver Dis 2001;21(3):427–436. [PubMed: 11586470]
7. Iredale JP, Benyon RC, Pickering J, et al. Mechanisms of spontaneous resolution of rat liver fibrosis. Hepatic stellate cell apoptosis and reduced hepatic expression of metalloproteinase inhibitors. J Clin Invest 1998;102(3):538–549. [PubMed: 9691091]

8. Oakley F, Meso M, Iredale JP, et al. Inhibition of inhibitor of kappaB kinases stimulates hepatic stellate cell apoptosis and accelerated recovery from rat liver fibrosis. Gastroenterology 2005;128(1):108–120. [PubMed: 15633128]
9. Wright MC, Issa R, Smart DE, et al. Gliotoxin stimulates the apoptosis of human and rat hepatic stellate cells and enhances the resolution of liver fibrosis in rats. Gastroenterology 2001;121(3): 685–698. [PubMed: 11522753]
10. Anan A, Baskin-Bey ES, Bronk SF, Werneburg NW, Shah VH, Gores GJ. Proteasome inhibition induces hepatic stellate cell apoptosis. Hepatology 2006;43(2):335–344. [PubMed: 16440346]
11. Anan A, Baskin-Bey ES, Isomoto H, et al. Proteasome inhibition attenuates hepatic injury in the bile duct-ligated mouse. Am J Physiol Gastrointest Liver Physiol 2006;291(4):G709–G716. [PubMed: 16798723]
12. Danial NN, Korsmeyer SJ. Cell death: critical control points. Cell 2004;116(2):205–219. [PubMed: 14744432]
13. Taylor RC, Cullen SP, Martin SJ. Apoptosis: controlled demolition at the cellular level. Nat Rev Mol Cell Biol 2008;9(3):231–241. [PubMed: 18073771]
14. Youle RJ, Strasser A. The BCL-2 protein family: opposing activities that mediate cell death. Nat Rev Mol Cell Biol 2008;9(1):47–59. [PubMed: 18097445]
15. Adams JM, Huang DC, Strasser A, et al. Subversion of the Bcl-2 life/death switch in cancer development and therapy. Cold Spring Harb Symp Quant Biol 2005;70:469–477. [PubMed: 16869785]
16. Lindsten T, Ross AJ, King A, et al. The combined functions of proapoptotic Bcl-2 family members bak and bax are essential for normal development of multiple tissues. Mol Cell 2000;6(6):1389–1399. [PubMed: 11163212]
17. Wei MC, Zong WX, Cheng EH, et al. Proapoptotic BAX and BAK: a requisite gateway to mitochondrial dysfunction and death. Science 2001;292(5517):727–730. [PubMed: 11326099]
18. Green DR. Apoptotic pathways: ten minutes to dead. Cell 2005;121(5):671–674. [PubMed: 15935754]
19. Willis SN, Adams JM. Life in the balance: how BH3-only proteins induce apoptosis. Curr Opin Cell Biol 2005;17(6):617–625. [PubMed: 16243507]
20. Traenckner EB, Wilk S, Baeuerle PA. A proteasome inhibitor prevents activation of NF-kappa B and stabilizes a newly phosphorylated form of I kappa B-alpha that is still bound to NF-kappa B. Embo J 1994;13(22):5433–5441. [PubMed: 7957109]
21. Karin M, Lin A. NF-kappaB at the crossroads of life and death. Nat Immunol 2002;3(3):221–227. [PubMed: 11875461]
22. Fernandez Y, Verhaegen M, Miller TP, et al. Differential regulation of noxa in normal melanocytes and melanoma cells by proteasome inhibition: therapeutic implications. Cancer Res 2005;65(14): 6294–6304. [PubMed: 16024631]
23. Fribley AM, Evenchik B, Zeng Q, et al. Proteasome inhibitor PS-341 induces apoptosis in cisplatin-resistant squamous cell carcinoma cells by induction of Noxa. J Biol Chem 2006;281(42):31440–31447. [PubMed: 16928686]
24. Gomez-Bougie P, Wuilleme-Toumi S, Menoret E, et al. Noxa up-regulation and Mcl-1 cleavage are associated to apoptosis induction by bortezomib in multiple myeloma. Cancer Res 2007;67(11):5418–5424. [PubMed: 17545623]
25. Perez-Galan P, Roue G, Villamor N, Campo E, Colomer D. The BH3-mimetic GX15-070 synergizes with bortezomib in mantle cell lymphoma by enhancing Noxa-mediated activation of Bak. Blood 2007;109(10):4441–4449. [PubMed: 17227835]
26. Qin JZ, Xin H, Sitailo LA, Denning MF, Nickoloff BJ. Enhanced killing of melanoma cells by simultaneously targeting Mcl-1 and NOXA. Cancer Res 2006;66(19):9636–9645. [PubMed: 17018621]
27. Chen L, Willis SN, Wei A, et al. Differential targeting of prosurvival Bcl-2 proteins by their BH3-only ligands allows complementary apoptotic function. Mol Cell 2005;17(3):393–403. [PubMed: 15694340]
28. Xu L, Hui AY, Albanis E, et al. Human hepatic stellate cell lines, LX-1 and LX-2: new tools for analysis of hepatic fibrosis. Gut 2005;54(1):142–151. [PubMed: 15591520]

29. Taimr P, Higuchi H, Kocova E, Rippe RA, Friedman S, Gores GJ. Activated stellate cells express the TRAIL receptor-2/death receptor-5 and undergo TRAIL-mediated apoptosis. Hepatology 2003;37(1):87–95. [PubMed: 12500193]

30. Barreyro FJ, Kobayashi S, Bronk SF, Werneburg NW, Malhi H, Gores GJ. Transcriptional regulation of Bim by FoxO3A mediates hepatocyte lipoapoptosis. J Biol Chem 2007;282(37): 27141–27154. [PubMed: 17626006]

31. Kobayashi S, Lee SH, Meng XW, et al. Serine 64 phosphorylation enhances the antiapoptotic function of Mcl-1. J Biol Chem 2007;282(25):18407–18417. [PubMed: 17463001]

32. Hackbarth JS, Lee SH, Meng XW, Vroman BT, Kaufmann SH, Karnitz LM. S-peptide epitope tagging for protein purification, expression monitoring, and localization in mammalian cells. Biotechniques 2004;37(5):835–839. [PubMed: 15560139]

33. Griffiths GJ, Dubrez L, Morgan CP, et al. Cell damage-induced conformational changes of the pro-apoptotic protein Bak in vivo precede the onset of apoptosis. J Cell Biol 1999;144(5):903–914. [PubMed: 10085290]

34. Perez-Galan P, Roue G, Villamor N, Montserrat E, Campo E, Colomer D. The proteasome inhibitor bortezomib induces apoptosis in mantle-cell lymphoma through generation of ROS and Noxa activation independent of p53 status. Blood 2006;107(1):257–264. [PubMed: 16166592]

35. Wang Q, Mora-Jensen H, Weniger MA, et al. ERAD inhibitors integrate ER stress with an epigenetic mechanism to activate BH3-only protein NOXA in cancer cells. Proc Natl Acad Sci U S A 2009;106(7):2200–2205. [PubMed: 19164757]

36. Nikiforov MA, Riblett M, Tang WH, et al. Tumor cell-selective regulation of NOXA by c-MYC in response to proteasome inhibition. Proc Natl Acad Sci U S A 2007;104(49):19488–19493. [PubMed: 18042711]

37. Elsharkawy AM, Oakley F, Mann DA. The role and regulation of hepatic stellate cell apoptosis in reversal of liver fibrosis. Apoptosis 2005;10(5):927–939. [PubMed: 16151628]

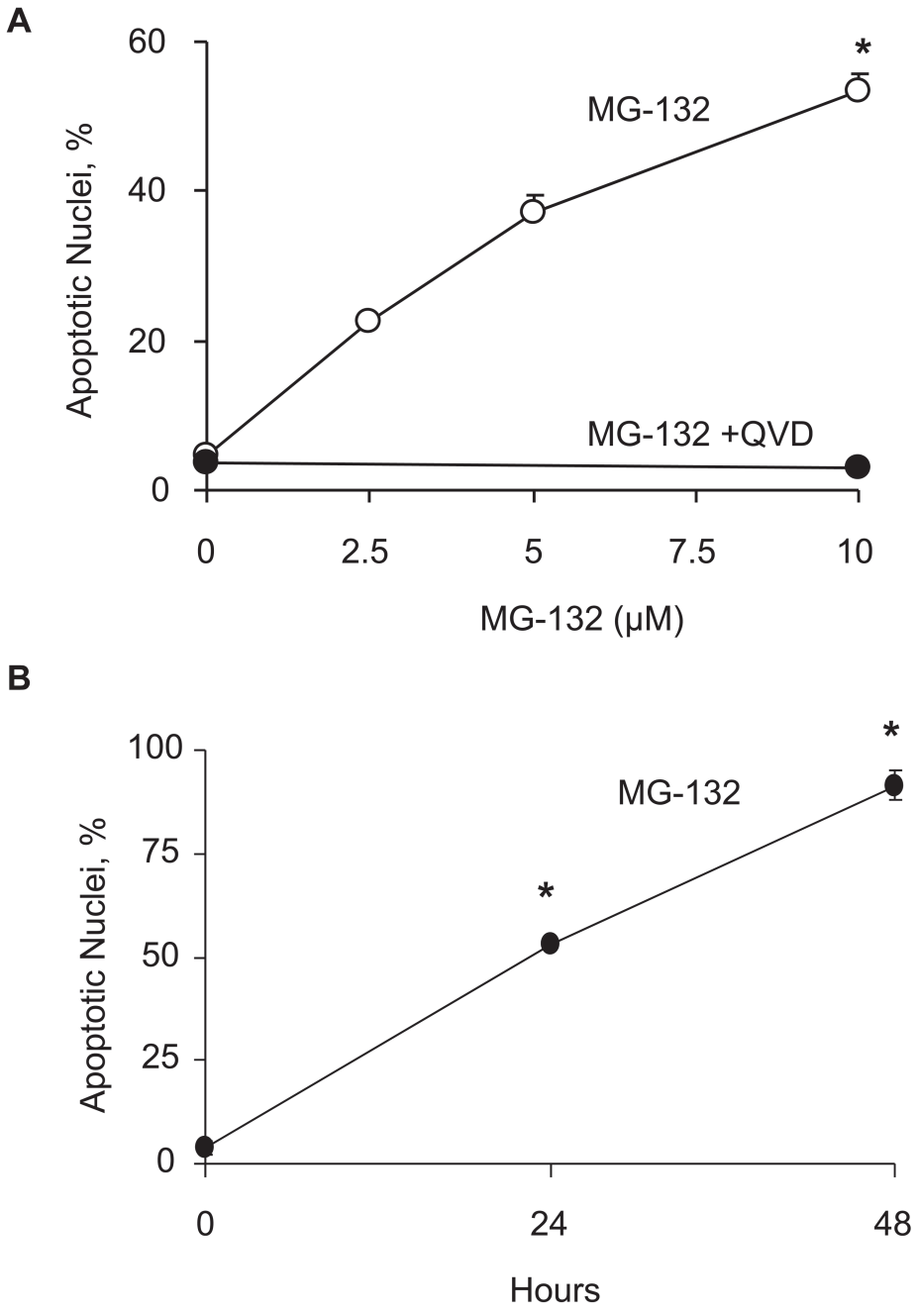

Figure 1. MG-132 induces apoptosis in LX-2 cells, which is inhibited by pan-caspase inhibitor

(A) LX-2 cells were incubated for 24 hours in the presence of increasing concentrations of MG-132 (0, 2.5, 5, 10 μmol/L) and in the presence of the pan-caspase inhibitor QVD at 5 μmol/L for 24 hours. MG-132 and QVD were prepared in DMSO as a vehicle. All data were expressed as mean ± standard error from three individual experiments. * $p < 0.01$ (10 μmol/L MG-132 treated cells vs. 10 μmol/L MG-132 plus QVD treated cells) (B) LX2 cells were treated by MG-132 (10 μmol/L) for indicated time. * $p < 0.01$ (MG-132 treated cells vs. vehicle treated cells)

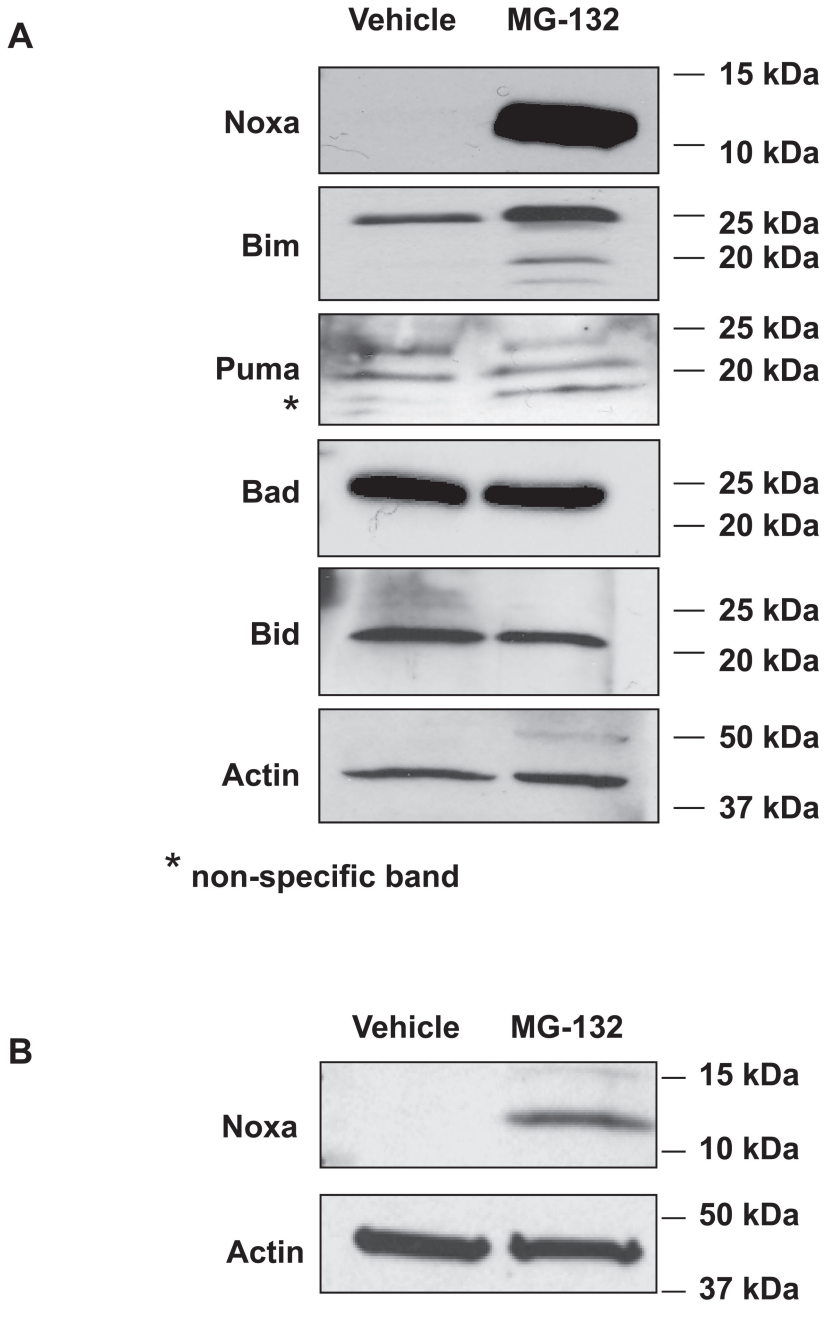

Figure 2. MG-132 induces expression of Noxa protein in LX-2 cells and rat primary HSC cells

(A) LX-2 cells were treated with MG-132 at 10 μmol/L for 24 hours, and a vehicle (DMSO) was used as control in the absence of MG-132. Cells were lysed and subjected to immunoblot analysis for indicated proteins. Actin was used as control for protein loading. (B) Rat primary HSC were treated with MG-132 10 μmol/L for 24 hours and subjected to immunoblot analysis using anit-Noxa.

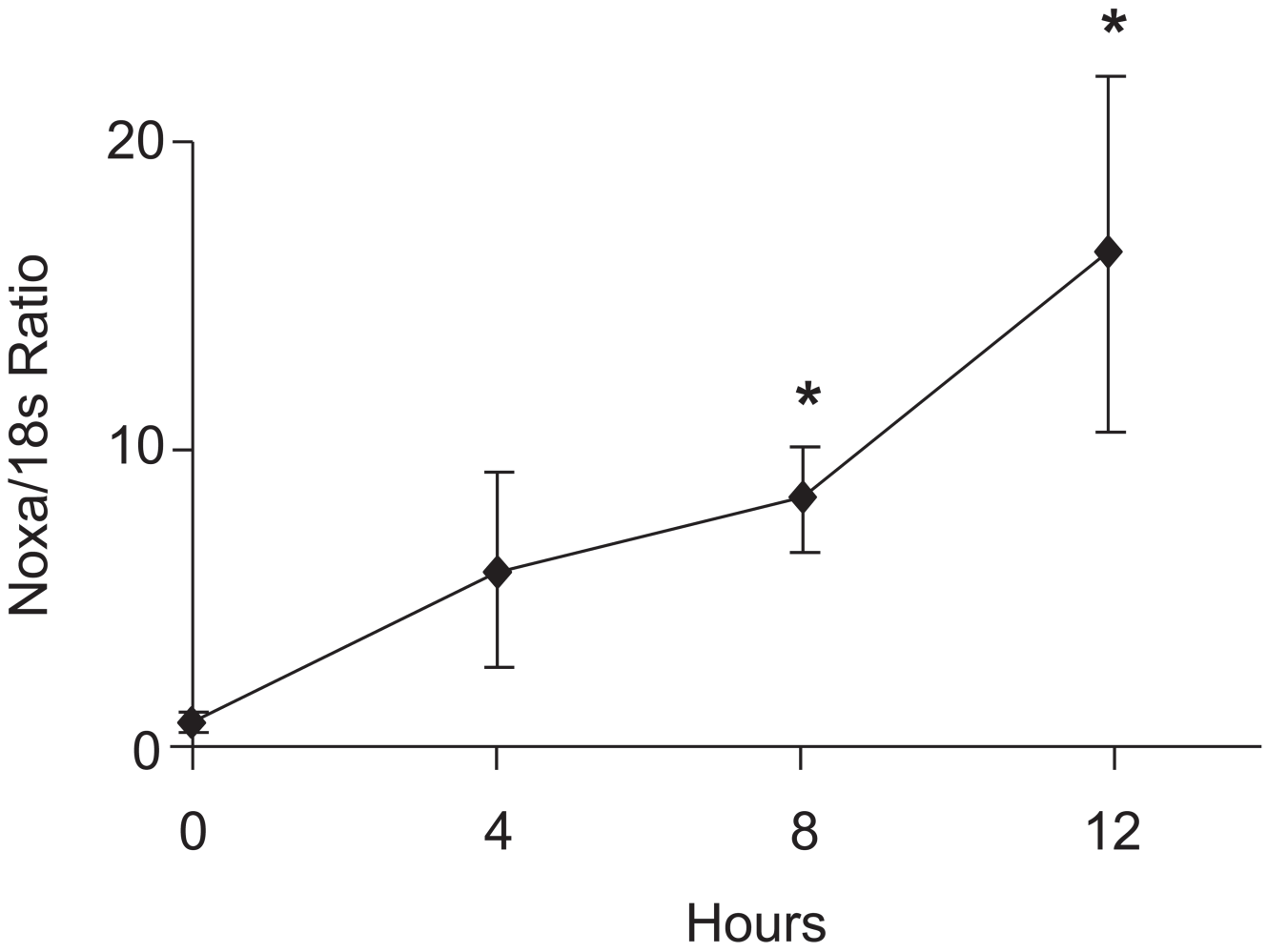

Figure 3. Noxa mRNA expression increases after treatment with MG-132

LX-2 cells were treated in the presence and absence of MG-132 at 10 μmol/L for indicated time. Total cellular RNA was extracted and analyzed by quantitative real-time PCR. Fold induction was determined after normalization to 18S housekeeping gene. All data represent the mean ± standard error of three separate experiments. * $p < 0.05$ (MG-132 treated cells vs. vehicle treated cells)

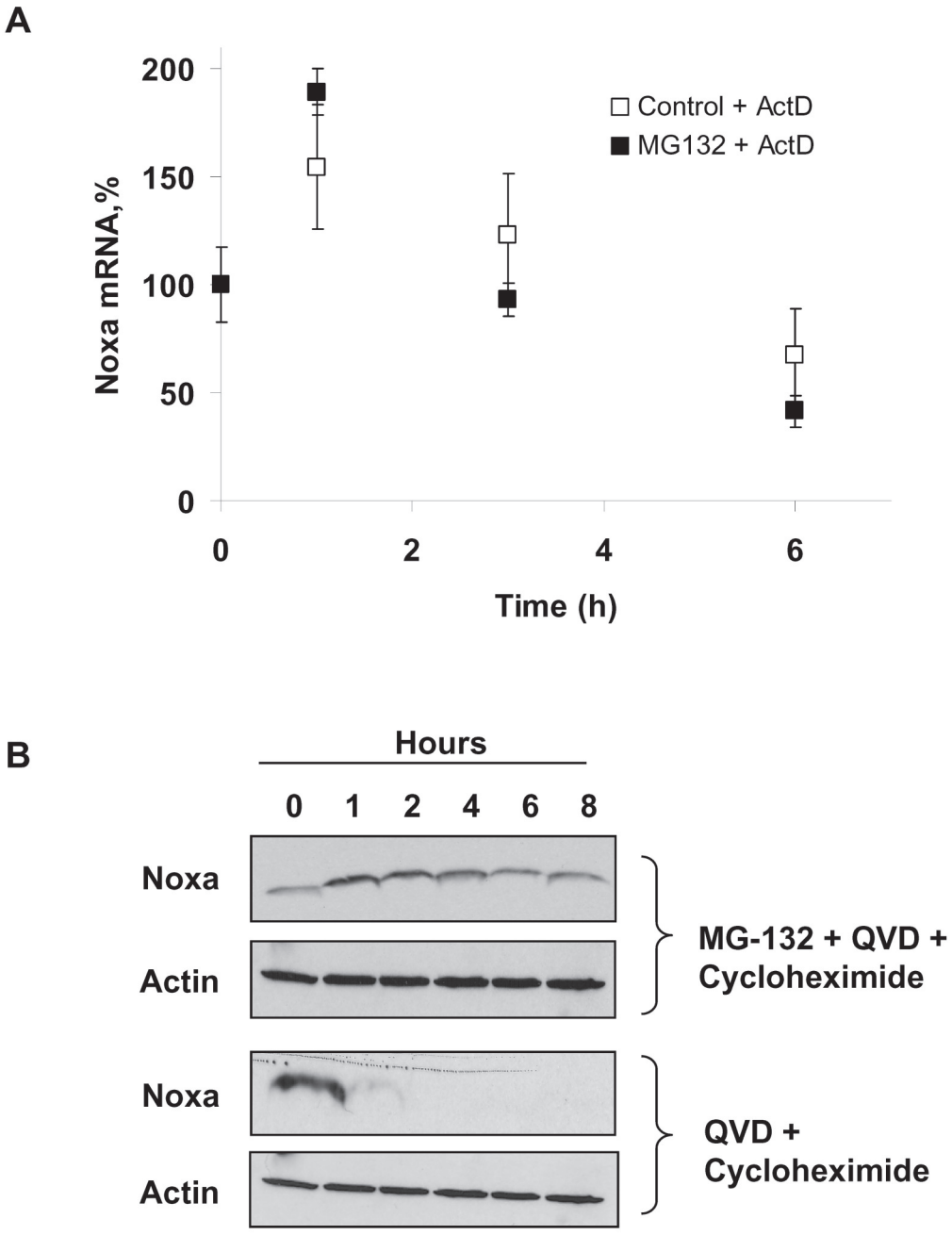

Figure 4. MG-132 effect on Noxa mRNA and protein half-life

(A) LX-2 cells were treated with Actinomycin D at 5 μmol/L and MG-132 at 10 μmol/L or vehicle for the indicated times and Noxa mRNA was quantified by RT-PCR. Noxa mRNA levels are expressed as a percent of signal compared to time zero. Data are mean +/− standard error from three samples, and are representative of three independent exeriments. (B) Cells were treated in the presence of the protein synthesis inhibitor cyclohexamide 20 μmol/L plus QVD at 5 μmol/L and the presence and absence of MG-132 at 10 μmol/L for the indicated time. Cells were lysed and subjected to immunoblot analysis for anti-Noxa. Actin was used as control for protein loading.

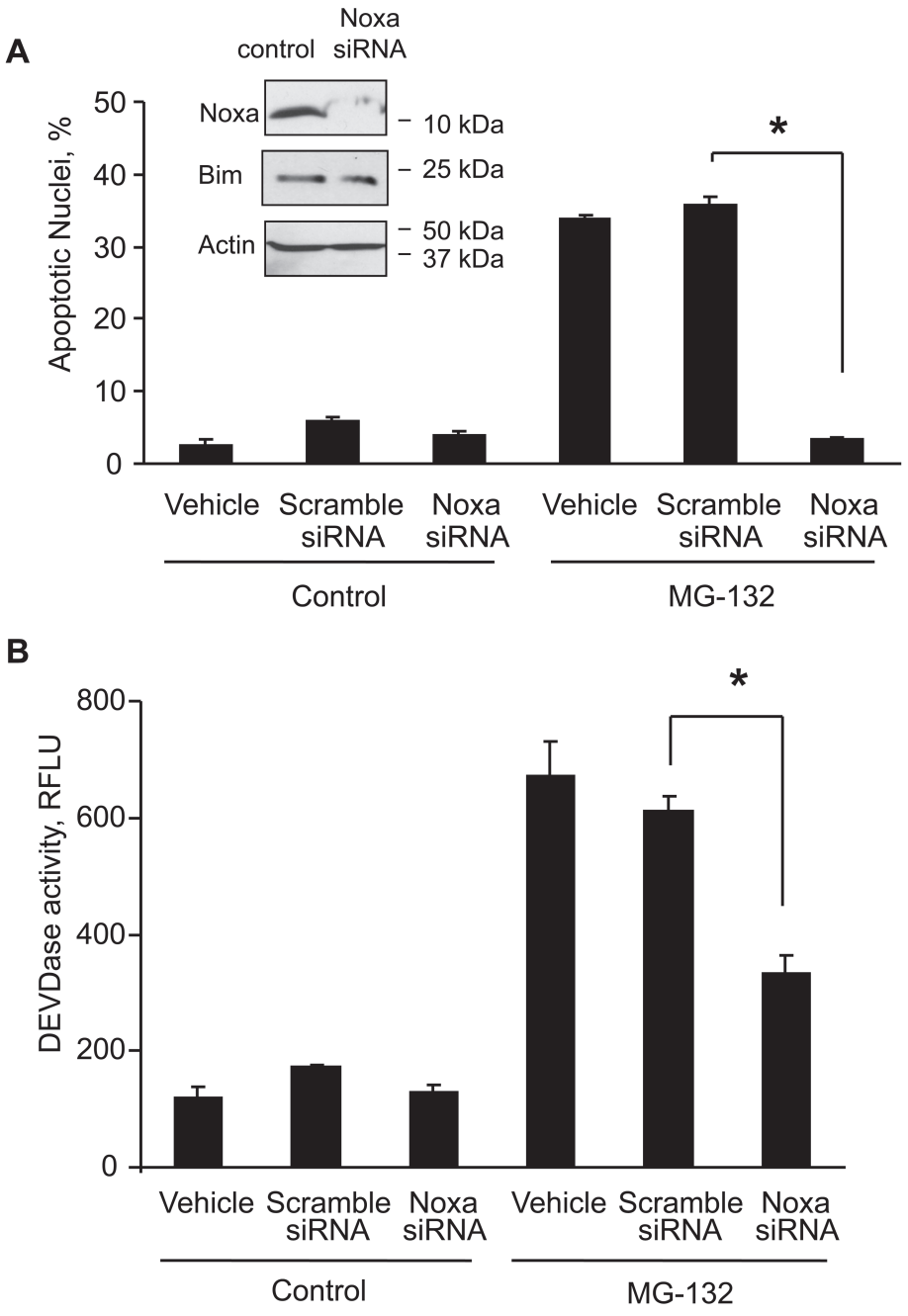

Figure 5. Noxa is essential for apoptosis by proteasome inhibition

(A) LX-2 cells were transiently transfected with a specific small-interfering RNA (siRNA) construct targeting Noxa or a control siRNA (scramble) for 24 hours; next cells were treated in the presence of MG-132 at 10 μmol/L for 24 hours. (A) Apoptosis was quantified using DAPI staining and fluorescence microscopy. Data were expressed as mean ± standard error from three individual experiments. * $p < 0.05$ (Noxa siRNA plus MG-132 treated cells vs. scramble siRNA plus MG-132 treated cells) (B) In parallel studies, apoptosis was also assessed by measuring caspase-3/7 activity. * $p < 0.05$ (Noxa siRNA plus MG-132 treated cells vs. scramble siRNA plus MG-132 treated cells)

A

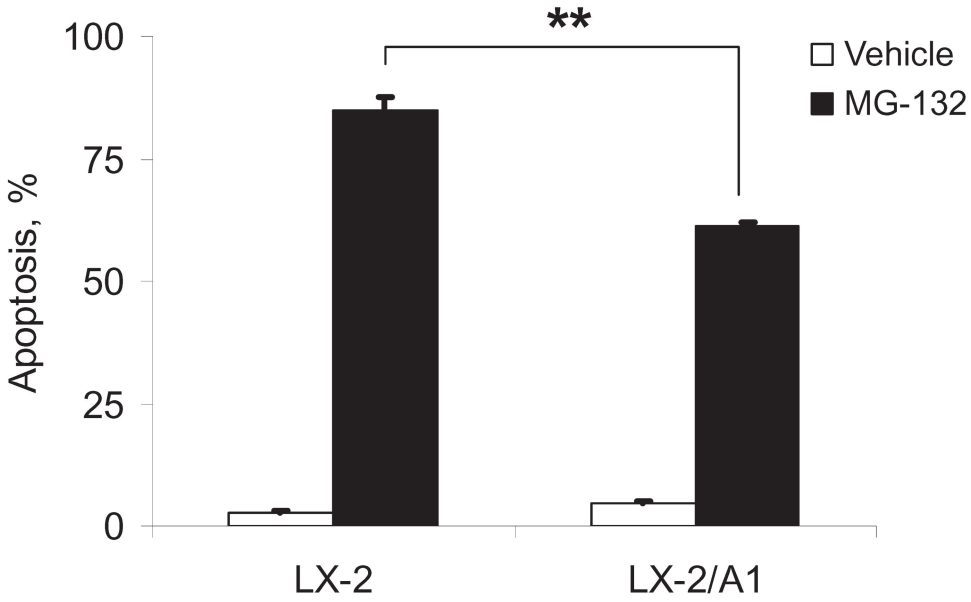

B

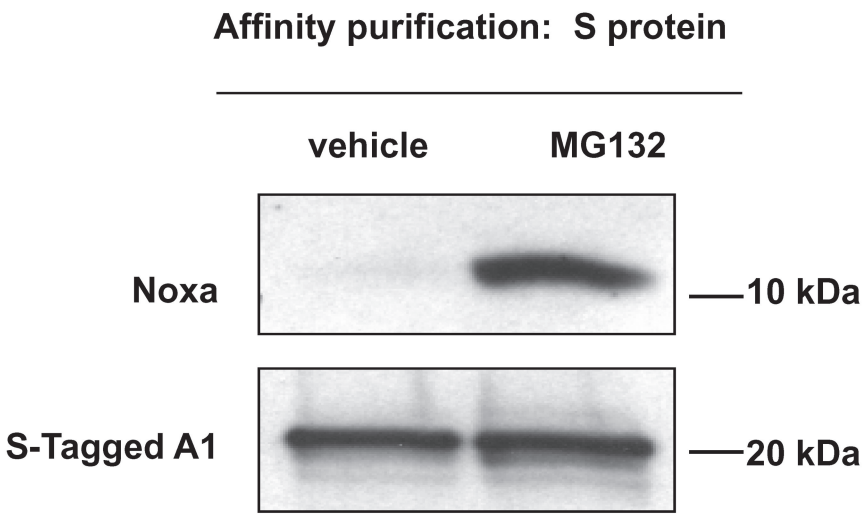

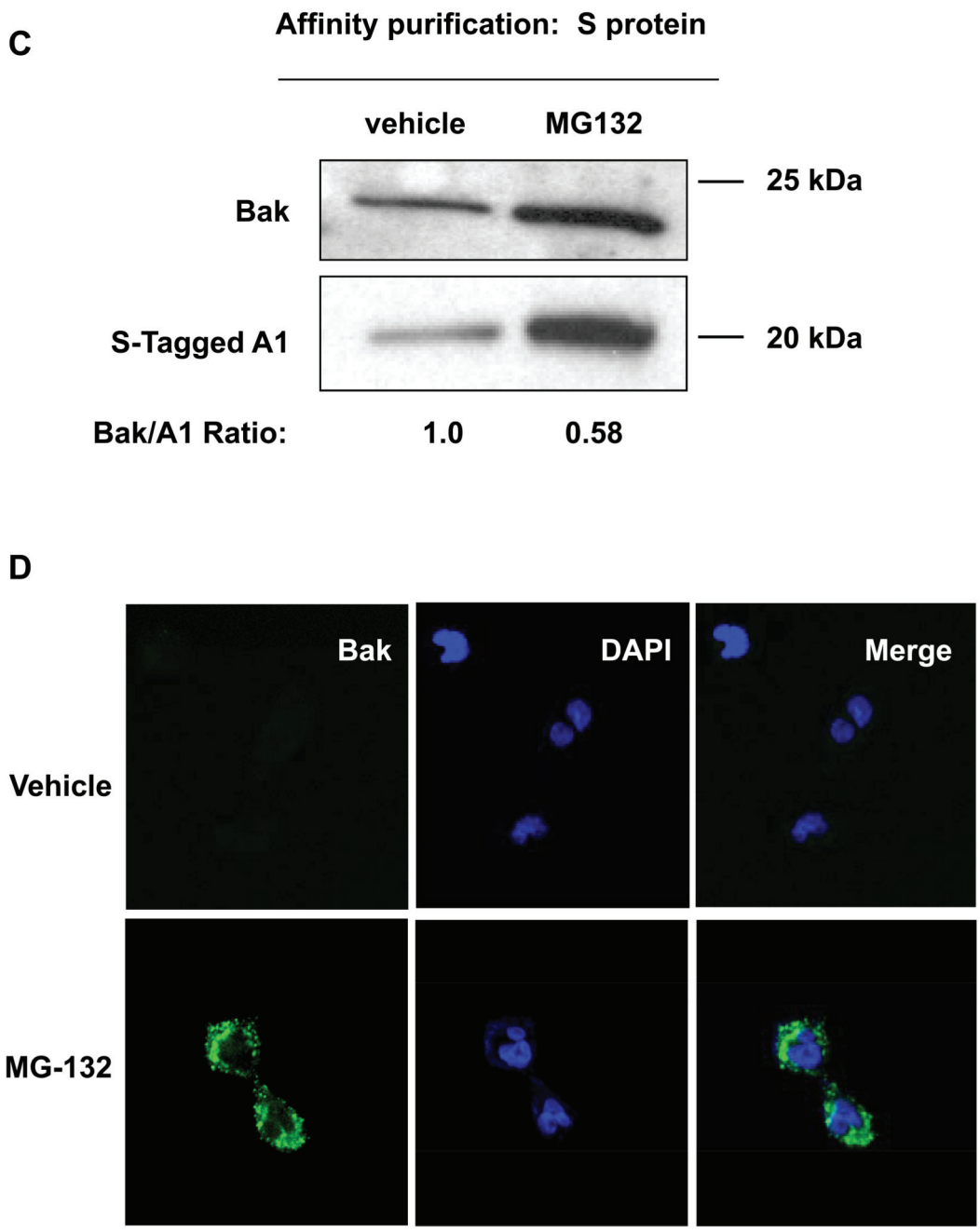

Figure 6. A1 is functionally inhibited by MG-132 treatment and Noxa association

(A) LX-2 cells stably transfected with S peptide-tagged A1 (LX-2/A1) or parental LX-2 cells were treated with vehicle (DMSO) or MG-132 (10 μmol/L) for 24 hours followed by DAPI nuclear staining. The percent of cells with apoptotic nuclear morphology was quantified and expressed as mean +/− SEM. ** = $p<0.01$ by ANOVA with post-hoc correction. (B) Noxa associates with S peptide-tagged A1 upon MG-132 treatment. LX-2/A1 cells were treated with the presence and absence of MG-132 at 10 μmol/L for 12 hours. Whole cell lysates were prepared, S peptide-tagged A1 was pulled down using S protein-agarose beads. S tagged-peptide A1 was removed from the beads by boiling in Laemnli sample buffer and resolved by SDS-PAGE. Immunoblot analysis was employed to identify

S peptide-tagged A1 and Noxa. (C) Affinity purified complexes prepared as in panel B from LX-2/A1 cells were probed with antisera to Bak and A1. (D) Proteasome inhibitor induces Bak activation. Cells were treated with either vehicle or MG-132 at 10 μmol/L for 12 hours and were subjected to Bak immunofluorescence study using antiserum specific for the N terminus of Bak. Upon Bak activation, this epitope is no longer masked within the protein and becomes available for antibody binding upon Bak conformational change.